Sterically restricted tin-phosphines, stabilized by weak intramolecular donor-acceptor interactions

Kasun S. Athukorala Arachchige, Paula Sanz Camacho, Matthew J. Ray, Brian A. Chalmers, Fergus R. Knight, Sharon E. Ashbrook, Michael Bühl, Petr Kilian, Alexandra M. Z. Slawin, J. Derek Woollins*

EaSTCHEM, School of Chemistry, University of St Andrews, St Andrews, Fife, KY16 9ST (UK) Fax: (+44) 1334 463384; E-mail: jdw3@st-andrews.ac.uk

KEYWORDS peri-substitution, donor-acceptor, intramolecular, tin, phosphorus, X-ray crystallography, DFT Calculations, Solid-state NMR

Supporting Information Placeholder

ABSTRACT: Four related sterically restricted *peri*-substituted acenaphthenes have been prepared containing mixed tin-phosphorus moieties in the proximal 5,6-positions (Acenap[SnR_3][P^iPr_2]; Acenap = acenaphthene-5,6-diyl; R_3 = Ph_3 (**1**), Ph_2Cl (**2**), Me_2Cl (**3**), Bu_2Cl (**4**)). The degree of intramolecular P-Sn bonding within the series was investigated by X-ray crystallography, solution and solid-state NMR spectroscopy and density functional theory (DFT/B3LYP/SBKJC/PCM) calculations. All members of the series adopt a conformation such that the phosphorus lone-pair is located directly opposite the tin centre, promoting an intramolecular donor-acceptor P→Sn type interaction. The extent of covalent bonding between Sn and P is found to be much greater in triorganotin chlorides **2**-**4** compared with triphenyl derivative **1**. Coordination of a highly electronegative chlorine atom naturally increases the Lewis acidity of the tin centre, enhancing the lp(P)−σ*(Sn−Y) donor-acceptor 3c-4e type interaction, as indicated by conspicuously short Sn-P *peri*-distances and significant $^1J(^{31}P,^{119}Sn)$ spin-spin coupling constants (SSCCs) in the range 740-754 Hz. Evidence supporting the presence of this interaction was also found in solid-state NMR spectra of some of the compounds which exhibit an indirect spin-spin coupling on the same order of magnitude as observed in solution. DFT calculations confirm the increased covalent bonding between P and Sn in **2**-**4**, with notable WBIs of *ca*. 0.35 obtained, compared to 0.1 in **1**.

INTRODUCTION

When large heteroatoms are constrained in sterically restricted systems, at distances well within the sum of their van der Waals radii, the degree of orbital overlap and the nature of the functional groups involved can determine whether the non-bonded intramolecular interactions that ensue are either repulsive due to steric hindrance or attractive as a result of weak or strong bonding.[1] Rigid polycyclic aromatic hydrocarbon backbones naphthalene[2] and acenaphthene[3] provide such spacial proximity of atoms or groups, with a double substitution at the close contact *peri*-positions ensuring the interacting atoms, are located in unavoidably congested environments.[4,5]

Whilst two hydrogen atoms (sum of the van der Waals radii (Σr_{vdW}) of two hydrogen atoms = 2.18 Å)[6] can be accommodated comfortably at the adjacent *peri*-positions in these systems (*peri*-distances 2.5/2.7 Å, respectively),[2,3] when larger heteroatoms are constrained in such cramped environments they naturally experience considerable steric hindrance. The repulsion between these bulky groups or atoms often results in the usually rigid naphthalene backbone deforming away from the ideal structure through in- and out-of-plane distortions of the exocyclic peri-bonds or buckling of the organic framework.[4,5,7,8] The unique feature of *peri*-substituted systems, however, is their ability to relieve steric strain and achieve a relaxed geometry via the formation of a direct bond between the *peri*-atoms.[5,9] The unique competition between attractive bonding interactions and steric repulsion in these systems accounts for their unusual reactivity and structure,[4,5,10] but whilst the nature of the intramolecular interactions in clear-cut cases is unambiguous, there are many examples which arouse conflicting interpretations of the bonding situation, with arguments for and against the existence of attractive forces and contention over whether or not the *peri*-atoms are linked by a chemical bond.[11-15]

This is typified by the controversial debate surrounding the potential occurrence of hypercoordination resulting from intramolecular bond formation in species containing the 8-dimethylaminonaphth-1-yl (DAN) fragment.[11-15] In these systems, the basic NMe_2 group is ideally located for donating its lone-pair electrons to, typically, a phosphorus or silicon functional group situated at the adjacent *peri*-position, with the strength of the interaction influenced by the Lewis acidity of the acceptor atom and hence the electronegativity of the substituents attached to it. For instance, the presence of two 1,2-phenylenedioxy groups bound to the phosphorus atom in **A** (Figure 1) results in a P-N distance of 2.132(2) Å and octahedral coordination at P, indicative of a strongly covalent intramolecular N→P dative bond.[13] In contrast, the degree of bonding in many other DAN-phosphines containing much weaker (i.e. longer) N···P interactions is much more vague (for example **B**; Figure 1),[14] with some authors claiming the formation of a dative intramolecular bond and associated hypercoordination in this case is highly unlikely, despite reports to the contrary based on N···P distances being significantly shorter than the sum of van der Waals radii.[11-15]

Many examples of *peri*-substituted systems stabilized by similar weak intramolecular donor-acceptor interactions between two electronically disparate functional groups have been reported,[5,8,16,17] including the first room temperature stable phosphine-phosphine donor-acceptor complex (**C** Figure1)[18] and a rare series of pentacoordinated nitrogen-tin species (**D** Figure1).[19] During our own investigations it emerged that in systems containing

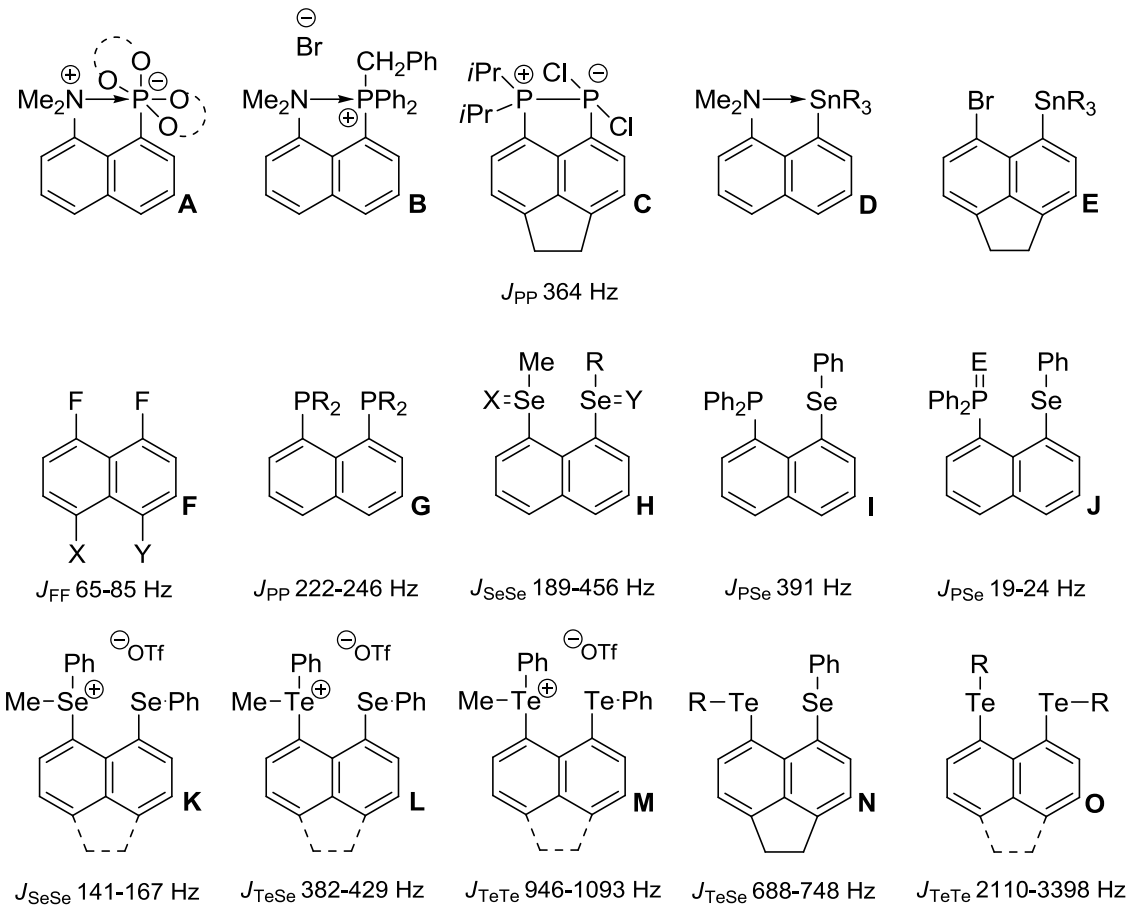

Figure 1. *Peri*-substituted systems stabilized by intramolecular donor-acceptor interactions across the *peri*-gap.

pnictogen and chalcogen moieties in the *peri*-positions, steric repulsion can be partly counterbalanced by attractive intramolecular interactions.[20-28] In particular, with heavier congeners such as tellurium occupying the proximal positions (**K**-**O** Figure 1),[20,22,25-28] but still formally nonbonded "across-the-bay", distances significantly shorter than the sum of the van der Waals radii were achieved. Wiberg bond indices (WBIs)[29] of up to *ca*. 0.18 computed for these separations indicate a significant degree of covalency between the *peri*-substituents in these systems, and under appropriate geometric conditions this can be traced back to weak donor–acceptor type interactions and the onset of 3-center-4-electron (3c4e) bonding.[20,22,25-28] Similar weak donor-acceptor interactions were observed during a recent study of sterically crowded bromine-tin derivatives (**E** Figure1), which became more prevalent with the increasing Lewis acidity of the tin centre as a result of contrasting substituent effects.[24]

In conjunction with X-ray structural data, indirect spin-spin coupling constants (SSCCs) present a convenient method for analyzing the extent of chemical bonding between two atoms. When NMR active nuclei are located within a molecule at sub van der Waals distances but formally non-bonded, spin-spin coupling can additionally be transmitted via the polarization of the lone-pair electrons (through-space coupling). The magnitude of through-space coupling, which is dependent upon the spacial distribution of electron density between the coupling nuclei, thus provides a good indication of any covalent contributions to the intramolecular lone-pair bonding interaction.[30-34]

For instance, the exceptionally large $J(^{19}F,^{19}F)$ SSCCs observed in the series of *peri*-difluoronaphthalenes **F** (65-85 Hz) were attributed to a significant ^{19}F-^{19}F through-space interaction which was found to rely heavily on the internuclear separation.[32] Bis-phosphines of type **G**[33] and selenium derivatives of type **H**[34] exhibit similar lone-pair interactions across the *peri*-gap, with $^4J(^{31}P,^{31}P)$ coupling constants in the former (222-246 Hz) of the same magnitude as ^1J-couplings for conventional P-P bonds (*cf*. **C** 364 Hz)[18] and the substantial $J(^{77}Se,^{77}Se)$ value for the O=Se···Se=O derivative (456 Hz) in the latter the largest known value for ^4J-coupling between two formally nonbonded Se atoms.[34] We have reported similar coupling between chalcogen atoms in bis-selenium (**K** 141-167 Hz) and mixed tellurium-selenium (**L** 382-429 Hz) cationic salts, with greater coupling observed for the heavier bis-tellurium derivatives (**M** 946-1093 Hz).[25] Even larger SSCCs are observed in the neutral mixed tellurium-selenium (**N** 688-748 Hz) and bis-tellurium (**O** 2110-3398 Hz) systems.[22,25-28]

The question now arises, how much of the observed spin-spin coupling in these sterically restrained systems is transmitted via the overlapping lone-pairs and how much is due to the polarized electrons in the succession of bonds that link the interacting nuclei. A good illustration of the through-space contribution to the overall coupling in these systems is found by comparing the $^4J(^{31}P,^{77}Se)$ coupling constant of phosphine **I** (391 Hz), in which the lone-pair on phosphorus is free to interact, with the value observed for equivalent phosphine oxides of type **J** (19-24 Hz) where the lone-pair is now taken up in the P=E double bond (E = S/Se).[21]

Phosphines (PR_3) are renowned as Lewis donors because of the availability of the lone-pair electrons which can be readily accept

Table 1. ^{31}P and ^{119}Sn NMR spectroscopy data.

	1	**2**	**3**	**4**
SnR_3	$SnPh_3$	$SnPh_2Cl$	$SnMe_2Cl$	$SnBu_2Cl$
Solution-state NMR				
^{31}P NMR	-31.5	-27.3	-24.4	-23.9
$J(^{31}P,^{119/117}Sn)$	373/355	754/721	742/709	740/707
^{119}Sn NMR	-183.7	-241.0	-143.1	-118.4
Solid-state NMR				
^{31}P NMR	-	-27.5	-27.4	-22.6
$J(^{31}P,^{119}Sn)$	-	850	669	730
^{119}Sn NMR	-	-265.3	-147.0	-137.8

All spectra run in $CDCl_3$; δ (ppm), J (Hz).

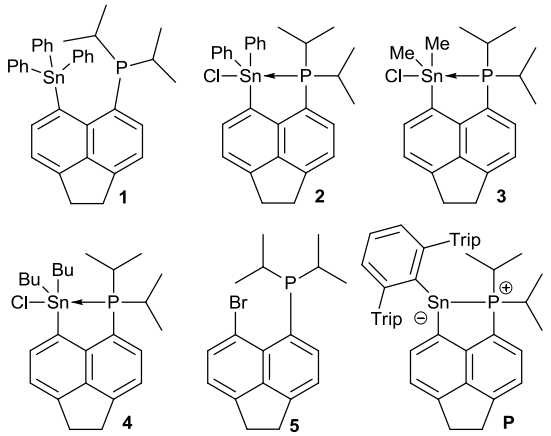

Figure 2. 6-diisopropylphosphinoacenaphth-5-yl-tin derivatives **1**-**4**, the bromine-phosphorus precursor **5** and previously reported Sn-P derivative **P**.[37]

ed by transition metals with vacant orbitals or non-metals such as the heavier trivalent group 15 halides.[18,35,36] We postulated that positioning the Lewis-basic P^{i}Pr$_2$ group across-the-bay from a comparatively electropositive tin functional group would afford sterically restricted systems, stabilized by intramolecular P→Sn donor-acceptor type interactions, similar to the previously reported Sn-P acenaphthene **P** (Figure 2).[37] In addition, as both *peri*-positions would be accommodated by NMR active nuclei, SSCCs could give a good indication of the extent of non-covalent bonding interactions present in these systems. In the present study, we investigate how the substituents around the tin centre affect the strength of the P→Sn donor-acceptor interactions and hence the value of SSCCs in a series of mixed Sn,P acenaphthenes Acenap(SnR_3)(P^{i}Pr$_2$) (R_3 = Ph_3 **1**; Ph_2Cl **2**; Me_2Cl **3**; Bu_2Cl **4**; Figure 2).

RESULTS AND DISCUSSION

Synthesis of 6-diisopropylphosphinoacenaphth-5-yl-tin derivatives 1-4: Mixed phosphorus-tin *peri*-substituted acenaphthenes [Acenap(SnR_3)(P^{i}Pr$_2$)] **1**-**4** were prepared through stepwise halogen-lithium exchange reactions of 5-(bromo)-6-(diisopropylphosphino)acenaphthene **5**.[18] For their synthesis, **5** was independently treated with a single equivalent of *n*-butyllithium in diethyl ether under an oxygen- and a moisture-free nitrogen atmosphere, at -78 °C, to afford the precursor 5-(lithio)-6-(diisopropylphosphino)acenaphthene. Addition of the respective triorganotin chloride [Ph_3ClSn, Ph_2Cl_2Sn, Me_2Cl_2Sn, Bu_2Cl_2Sn] subsequently afforded [Acenap($SnPh_3$)(P^{i}Pr$_2$)] (**1**), [Acenap($SnPh_2Cl$)(P^{i}Pr$_2$)] (**2**), [Acenap($SnMe_2Cl$)(P^{i}Pr$_2$)] (**3**) and [Acenap($SnBu_2Cl$)(P^{i}Pr$_2$)] (**4**) in moderate to good yield [72 (**1**), 65 (**2**), 46 (**3**), 93% (**4**); Scheme 1]. All four compounds were characterized by multinuclear magnetic resonance spectroscopies and mass spectrometry, and the homogeneity of the new compounds was where possible confirmed by microanalysis. ^{31}P and ^{119}Sn NMR spectroscopic data for the series of acenaphthene derivatives is displayed in Table 1. In addition, similar treatment of the phosphorus-lithium precursor of **5** with $SnCl_4$ afforded diaryltin dichloride [{Acenap(P^{i}Pr$_2$)}$_2$($SnCl_2$)] (**6**); the quality of the X-ray diffraction data, however, prevents publication and a discussion of this compound is omitted from this manuscript but a stick and ball representation can be found in the SI.

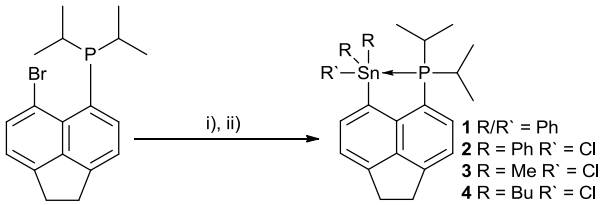

Scheme 1. The preparation of phosphorus-tin *peri*-substituted acenaphthenes **1**-**4**: (i) *n*BuLi (1 equiv), Et_2O, −78 °C, 2 h; (ii) Ph_3ClSn (**1**)/Ph_2Cl_2Sn (**2**)/Me_2Cl_2Sn (**3**)/Bu_2Cl_2Sn (**4**) (1 equiv), Et_2O, −78 °C, 1 h; RT, 16 h.

Solution- and Solid-state NMR spectroscopy: The ^{31}P NMR spectra for tin derivatives **1**-**4** exhibit single peaks with satellites attributed to ^{31}P-^{119}Sn and ^{31}P-^{117}Sn coupling. Consistent with a reduction in the electron density at the tin centre, ^{31}P NMR signals for triorganotin chlorides **2**-**4** (**2** -27.3, **3** -24.4, **4** -23.9) display a downfield shift compared to triphenyltin derivative **1** (-31.5). The relatively large J values observed in **1** for ^{31}P-$^{119/117}$Sn coupling (373/355 Hz) indicates a potential weakly attractive through-space interaction between the phosphorus lone-pair and the tin centre. Even larger $J(^{31}P,^{119/117}Sn)$ SSCCs are observed for triorganotin chlorides **2**-**4** (**2** 754/721 Hz; **3** 742/709 Hz; **4** 740/707 Hz), implying the donor-acceptor through-space P→Sn lone-pair interaction in these systems is much stronger, as expected from the enhanced electropositivity of the tin centre as a result of coordinating to a highly electronegative chlorine atom.

The ^{119}Sn NMR spectra for **1**-**4** all display doublets with the splitting attributed to $J(^{119}Sn,^{31}P)$ coupling. The NMR signal for triorganotin chloride **2** (-241.0 ppm) is shifted upfield compared to triphenyltin derivative **1** (-183.7 ppm) and within the series of triorganotin chlorides the signals are consistently low field shifted going from **2** (Ph_2Cl -241.0 ppm) to **3** (Me_2Cl –143.1 ppm) to **4** (Bu_2Cl -118.4 ppm).

^{31}P and ^{119}Sn solid-state NMR spectra were obtained for compounds **2**, **3** and **4**, and are shown in Figure 3. Crystal structures show just one crystallographically-distinct molecule in the asymmetric unit, suggesting a single ^{31}P and ^{119}Sn signal should be

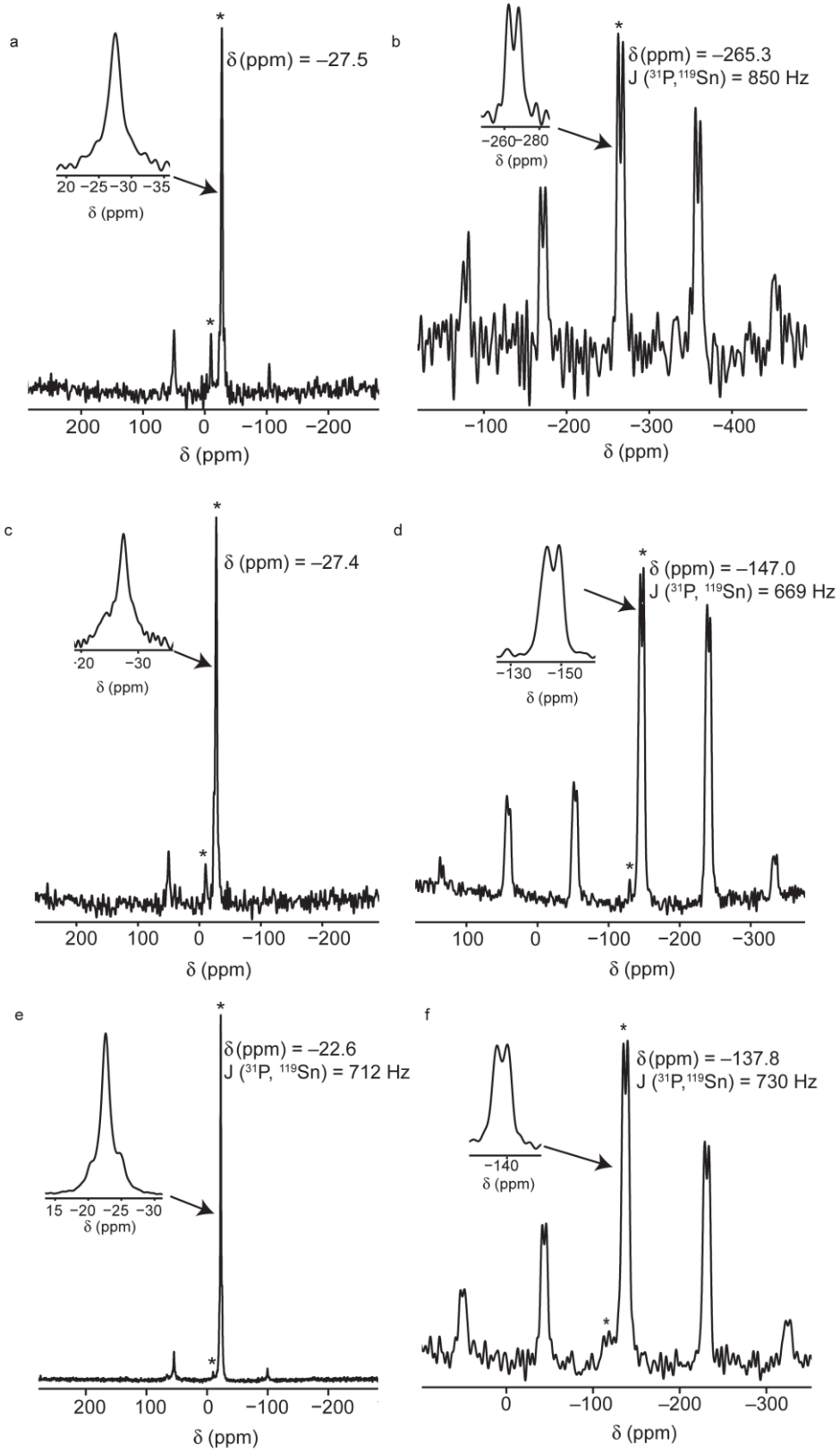

Figure 3. ^{31}P and ^{119}Sn MAS NMR spectra of compounds **2** (a/b), **3** (c/d) and **4** (e/f), respectively, acquired at B_0 = 9.4 T, using MAS rates of 12.5 kHz (^{31}P) and 14 kHz (^{119}Sn). For compounds **2** and **3** sensitivity in ^{119}Sn spectra was enhanced by the transfer of magnetization from ^{1}H using CP. The values quoted correspond to the isotropic chemical shift and the splitting observed in the isotropic peak. Isotropic resonance are indicated by *, the rest correspond to the spinning sidebands.

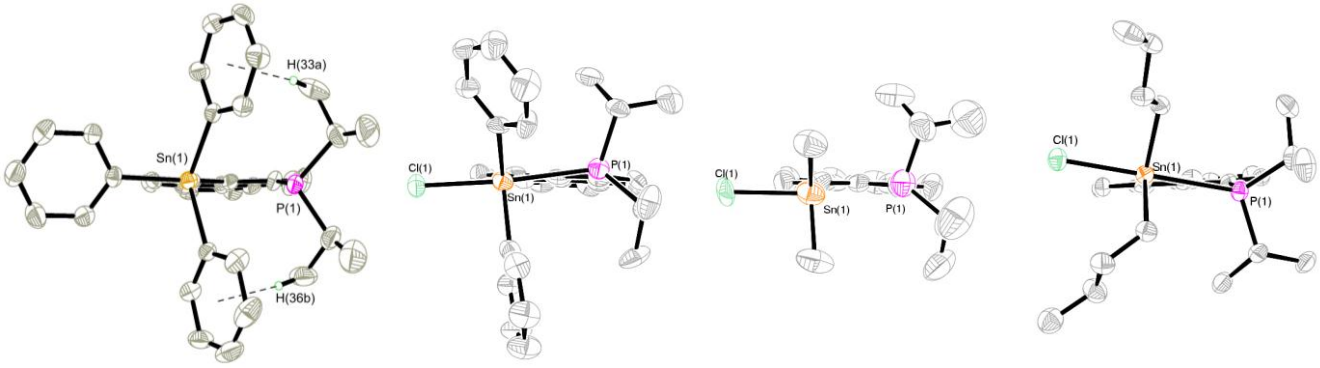

Figure 3. The molecular conformations of **1**-**4** (50% probability ellipsoids) showing the orientation of the substituents bound to Sn and P; **1** adopts a BAA-CC conformation with CH···π interactions between neighboring phenyl and isopropyl moieties whilst **2**-**4** adopt similar BAA-AC conformations.

observed in each case. However, in each ^{31}P spectrum a second isotropic resonance is observed at –9.5 ppm, corresponding to an unknown impurity.

For ^{119}Sn, a range of spinning sidebands are observed, reflecting the presence of a large chemical shift anisotropy (CSA). Owing to the lower sample volume, and therefore lower sensitivity, spectra for compounds **2** and **3** were acquired using CP experiments. In each case, each of the ^{119}Sn resonances signals is split into a clear doublet, with ^{1}J values of 850, 669 and 730 Hz for compounds **2**, **3** and **4**, respectively. This clearly demonstrates the presence of a significant indirect spin-spin coupling, on the same order of magnitude as observed in solution. For ^{31}P, a much smaller CSA is observed, with just two small spinning sidebands in each case. *J* couplings to ^{119}Sn, will appear as so-called "satellite" peaks, owing to the low natural abundance of ^{119}Sn, and this can be just resolved for compound **4**. The splitting measured has a significant uncertainty (of ±20 Hz) owing to the linebroadening present. Although these splittings are not fully resolved for compounds **2** and **3**, owing to the linebroadening observed, the spectral lineshapes are not inconsistent with the presence of couplings between 670-850 Hz to ^{119}Sn.

X-ray investigations: Suitable single crystals were obtained for **1** and **4** by recrystallisation from a saturated hexane solution of the respective compound. Crystals for **2** and **3** were obtained by diffusion of hexane into saturated THF and DCM solutions of the compounds, respectively. All five compounds crystallize with only one molecule in the asymmetric unit. Selected interatomic bond lengths and angles are listed in Tables 2-4. Further crystallographic information can be found in the Supporting Information.

The molecular structures of tin-phosphorus *peri*-substituted acenaphthenes **1**-**4** can be categorized using the classification systems devised by Nakanishi *et al*.[8] and Nagy *et al*.[38] and previously employed for related chalcogen and pnictogen systems.[20-22,25-28] Each Sn-Y/P-C_{iPr} substituent bond is designated as either type A (perpendicular), B (coplanar) or C (intermediate) depending upon the relative alignment with respect to the mean acenaphthene plane.[8] The absolute conformation of the *peri*-substituents is determined from C-C-Z-Y torsion angles θ, which define the degree of rotation around the Z-C_{Acenap} bonds (Table S3).[38]

Mono-systems **1**-**4** adopt similar conformations, classified as type BAA-CC for **1** and BAA-AC for **2**-**4** (Figure 3). In all four compounds, two Sn-C_R bonds align perpendicular to the mean acenaphthene plane (type A) with the alkyl groups displaced *trans* to one another on opposite sides of the molecule. The remaining Sn-C_{Ph} bond in **1** and the three Sn-Cl bonds of **2**-**4** subsequently align along the plane of the acenaphthene backbone (type B), giving rise to *quasi*-linear C_{Ph}-Sn···P and Cl-Sn-P three-body fragments in which angles approach 180° (**1** 177.63(1)°, **2** 171.62(9)°, **3** 168.93(8)°, **4** 171.23(3)°). In the triphenyltin derivative **1** the two P-C_{iPr} bonds occupy positions on different sides of the acenaphthene plane, each intermediate between an axial and equatorial configuration, described as type CC. The location of the two isopropyl groups, in close proximity to the two axial phenyl rings on Sn, is such that two intramolecular CH···π interactions exist to stabilize the compound, with H36B···Cg(13-18) and H33A···Cg(25-30) distances of 2.60 Å and 2.93 Å (Figure 3). No such interactions exist in triorganotin chlorides **2**-**4**, allowing the isopropyl groups to rotate around the P-C_{Acenap} bond and lie with an axial-twist configuration (type AC). Nevertheless, the overriding factor determining the molecular conformation of each compound is the location of the phosphorus lone-pair, which in all cases points directly at Sn on the opposite side of the *peri*-gap.

The *quasi*-linear alignment of the C_{Ph}-Sn···P and Cl-Sn-P three-body fragments in **1**-**4** therefore provides the correct geometry to promote delocalization of the phosphorus lone-pair (G) to an antibonding σ*(Sn−Y) orbital, forming an energy lowering, donor-acceptor three-centre four-electron (3c-4e) type interaction which helps to stabilize the molecule. Such, attractive, interactions which lead to *peri*-distances significantly shorter than the sum of van der Waals radii (**1** 3.2511(19) Å, **2** 2.815(3) Å, **3** 2.912(3) Å,**4** 2.8721(10) Å; r_{vdW}(SnP) 3.97 Å),[6] have been shown to partially counterbalance steric repulsion between heavier congeners in *peri*-substituted systems and thus play an important role in controlling their fine structures (G-dependence).[8,20-22,25-28]

The steric and electronic effects of substituents (Y) attached to the *peri*-atoms must also be considered however, as subtle changes to the size and donor/acceptor properties of Y can greatly influence the underlying bonding situation and thus the particular conformations that ensue (Y-dependence). This is aptly demonstrated by comparing the contrasting size of the *peri*-distance in triphenyltin derivative **1** (3.2511(19) Å) with the much smaller distances exhibited by triorganotin chlorides **2**-**4** (2.815(3) Å-2.912(3) Å), indicative of much stronger donor-acceptor interactions in the latter as a result of replacing a phenyl group with a highly electronegative chlorine atom, subsequently increasing the Lewis acidity of the tin centre.

Nonetheless, the non-bonded Sn···P distance in **1** (3.2511(19) Å) is still 18% shorter than the sum of van der Waals radii for P/Sn (3.97 Å) and a significant 3c-4e interaction is predicted to be present, similar in strength to the interactions reported in related, formally non-bonded, bis-tellurium systems in which Wiberg bond indices (WBIs) of around 0.15 have been computed. Even stronger 3c-4e bonding interactions are expected in **2**-**4** in which conspicuously short intramolecular Sn-P bond lengths are ~28% within the sum of van der Waals radii and approach the distance for a single electron pair (2c-2e) Sn-P covalent bond (2.63 Å).

Furthermore, with only one bonding pair of electrons available

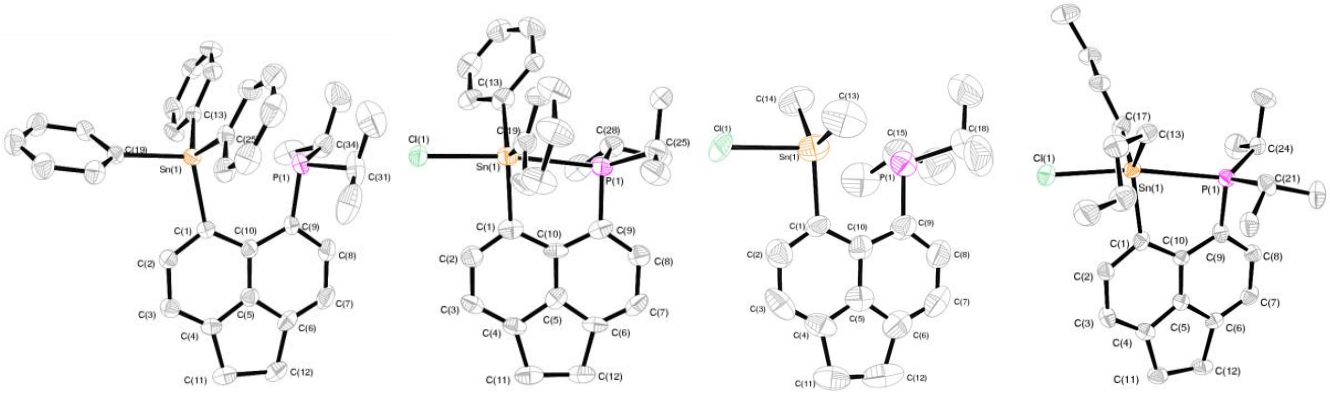

Figure 4. The molecular structures of **1**-**4**, (50% probability ellipsoids) showing the difference in in-plane distortion within the bay-region between the weakly bonded triphenyltin derivative **1,** and triorganotin chlorides **2**-**4**.

for the two bonds in hypervalent 3c-4e systems, donation of the phosphorus lone-pair into the σ*(Sn−Cl) is accompanied by a natural reduction of the Sn–Cl bond order, making the Sn-Cl bonds weaker and subsequently longer, extending from ~2.4 Å ($SnPh_2Cl_2$ 2.373(9) Å; $SnMe_2Cl_2$ 2.389(9) Å; $SnBu_2Cl_2$ 2.413(1) Å/2.4656(9) Å)[39] in the starting material triorganotin chlorides to 2.525(3) Å in **2**, 2.626(2) Å in **3** and 2.5317(9) Å in **4**. For comparison, the *quasi*-linear Br-Se-Se three-body fragment of related bromoselanyl cation [Acenap(SePh)(SePhBr)]$^+$, in which the Se-Se *peri*-distance is notably compressed (74% $\sum r_{vdW}$) is calculated to contain significant 3c-4e character, with substantial WBIs of 0.36 and 0.57 obtained for the Se-Se and Se-Br bonds, respectively.[23] The weaker C_{Ph}-Sn···P interaction present in triphenyltin **1** also exhibits notable weakening and lengthening of the equatorial C_{Ph}-Sn bond, although as expected to a much lesser extent, with distances extending from an average of 2.12 Å in Ph_3SnCl[39] to 2.187(6) Å for the C19-Sn1 bond (*c.f.* axial C13-Sn1 2.131(5) Å; axial C25-Sn1 2.151(6) Å).

Unsurprisingly, when large heteroatoms such as Sn and P are forced to occupy positions close in space, within the sum of their van der Waals radii, they experience severe steric hindrance. Such repulsive interactions are known to transpire between *peri*-substituents in naphthalenes and related systems and cause the carbon framework to distort away from an ideal geometry to minimize the steric strain. This occurs via in-plane and out-of-plane distortions of the exocyclic bonds and supplementary buckling of the aromatic ring system (angular strain).[4,5] Under certain geometrical constraints, however, as observed in **2**-**4** and to a lesser extent in **1**, steric strain can be relieved via the formation of an attractive intramolecular interaction between the *peri*-atoms due to the presence of weak or strong bonding.[8,9] The formation of an attractive 3c-4e Cl-Sn-P bond in triorganotin chlorides **2**-**4** therefore acts to counterbalance the steric repulsion between the Sn and P lone-pairs and is thus accompanied by a natural reduction in molecular distortion within the acenaphthene backbone. This is most apparent within the acenaphthene plane where a decrease in splay angle from 20.1° in a non-bonded tin-bromine analogue [Acenap(Br)($SnPh_3$)],[24] to 17.1 in **1** and 4.1°, 6.7° and 5.4° in **2**-**4** respectively, represents the bay region angles becoming more acute as the *peri*-atoms come together as a result of bond formation (Figure 4).

The tin centre in triphenyl derivative **1** adopts a distorted geometry intermediate between tetrahedral and trigonal bipyramidal (tbp), thanks in part to the additional intramolecular Sn···P interaction. As such, the sum of the C1-Sn1-C13, C1-Sn1-C25 and C13-Sn1-C25 bond angles (346.3°) for the *pseudo*-equatorial groups lies above that for an ideal tetrahedron (328.5°) but still less than that of a perfect trigonal bipyramid (360°). The phosphorus atom meanwhile, adopts a distorted trigonal pyramidal geometry with C-P-C angles compressed from an ideal 107° to an average of 101°. With much stronger Sn-P interactions operating in triorganotin chlorides **2**-**4**, the geometry around the tin centre moves more towards trigonal bipyramidal, with the sum of the *pseudo*-equatorial C-Sn-C bond angles increasing to 359° in all three compounds and the Sn atom lying only 0.13 Å from the C-C-C equatorial plane. Correspondingly, the phosphorus atom sits in a distorted tetrahedral environment, with C-P-C angles increasing to 105°-107°.

DFT Calculations: In order to probe how well the findings from X-ray structural analyses could be reproduced and rationalized computationally and specifically to assess the extent of three-centre, four-electron type interactions occurring in these tin-phosphorus systems, density functional theory (DFT) calculations were performed for all five compounds in this study. Atomic co-ordinates obtained from X-ray crystallography for **1**-**4** and **6** (see SI for the DFT results of the latter) were optimized at the B3LYP/SBKJC level, chosen for compatibility with our previous calculations on related tin-bromine species.[24] At this level, the optimized Sn-P *peri*-distances in **1**-**4** are appreciably overestimated compared to those observed in the solid by up to 0.2 Å (Table S7, ESI). All four compounds were reoptimised using the PCM implementation of Tomasi and co-workers,[40] using the same methods and basis sets previously employed (and employing the parameters of THF to model a moderately polar environment). Little change was observed for the unpolar structure **1**, with the Sn-P distance remaining substantially overestimated. A notable improvement was found for polar compounds **2**-**4**, however, with reoptimised Sn-P *peri*-distances now differing from those found experimentally in the solid by up to only 0.063 Å (Table 4).

From structural and spectroscopic analyses, the extent of covalent bonding (conveniently probed by the Wiberg Bond Index (WBI))[29] between tin and phosphorus in triorganotin chlorides **2**-**4** is predicted to be much greater than that found in triphenyltin derivative **1**. In these systems, coordination of a highly electronegative chlorine atom increases the Lewis acidity of the tin centre, naturally enhancing the lp(P)−σ*(Sn−Y) donor-acceptor interaction. This results in conspicuously short Sn-P *peri*-distances (**2** 2.815(3) Å, **3** 2.912(3) Å, **4** 2.8721(10) Å; *c.f.* **1** 3.2511(19) Å) and a concomitant increase in through-space spin-spin coupling, with large $J(^{31}P,^{119}Sn)$ values observed for **2**-**4** in the range 740-754 Hz (*c.f.* **1** 373 Hz). Substantial WBIs of up to 0.36 are found for **2**-**4**, much larger than that found for **1** (0.12), and whilst the latter is non-negligible and even suggests there is a significant degree of covalency between Sn and P in **1**, it indicates greater

multicentre bonding transpiring in the triorganotin chloride systems.

Table 2. Selected interatomic distances [Å] and angles [°] for 1-4

	1 - $SnPh_3$	**2 - $SnPh_2Cl$**	**3 - $SnMe_2Cl$**	**4 - $SnBu_2Cl$**
Peri-region-distances				
Sn(1)···P(1)	3.2511(19)	2.815(3)	2.912(3)	2.8721(10)
Σr_{vdW} - Sn···P[a]; % Σr_{vdW}[a]	0.7189; 82	1.155; 71	1.058; 73	1.0979; 72
Sn(1)-Cl(1)	-	2.525(3)	2.626(2)	2.5317(9)
Sn(1)-C(1)	2.172(6)	2.164(11)	2.171(9)	2.166(3)
P(1)-C(9)	1.834(6)	1.806(12)	1.820(10)	1.815(4)
Peri-region bond angles				
Sn(1)-C(1)-C(10)	127.1(4)	119.2(7)	121.6(6)	121.8(2)
C(1)-C(10)-C(9)	128.5(5)	128.1(9)	129.5(9)	127.1(3)
P(1)-C(9)-C(10)	122.2(4)	116.8(9)	115.6(7)	116.5(2)
Σ of bay angles	**377.8(8)**	**364.1(15)**	**366.7(13)**	**365.4(4)**
Splay angle[b]	17.8	4.1	6.7	5.4
C(4)-C(5)-C(6)	111.3(5)	111.1(9)	112.2(9)	111.8(3)
Out-of-plane displacement				
Sn(1)	-0.193(1)	-0.376(1)	-0.265(1)	-0.339(1)
P(1)	-0.275(1)	0.130(1)	0.142(1)	0.345(1)
Central naphthalene ring torsion angles				
C:(6)-(5)-(10)-(1)	178.9(5)	-177.8(9)	-178.4(9)	-174.5(3)
C:(4)-(5)-(10)-(9)	-179.6(5)	-179.8(8)	179.9(9)	-176.7(3)

[a] van der Waals radii used for calculations: r_{vdW}(Sn) 2.17 Å, r_{vdW}(P) 1.80 Å; [b] Splay angle: Σ of the three bay region angles – 360

Table 3. Bond angles [°] categorising the geometry around Sn and P in 1-4.

1		**2**		**3**		**4**	
C(1)-Sn(1)-C(13)	113.1(2)	**C(1)-Sn(1)-C(13)**	126.7(4)	**C(1)-Sn(1)-C(13)**	114.5(4)	**C(1)-Sn(1)-C(13)**	118.40(13)
C(1)-Sn(1)-C(19)	104.7(2)	**C(1)-Sn(1)-C(19)**	113.1(4)	**C(1)-Sn(1)-C(14)**	127.8(4)	**C(1)-Sn(1)-C(17)**	125.54(13)
C(1)-Sn(1)-C(25)	111.0(2)	**C(1)-Sn(1)-Cl(1)**	94.5(3)	**C(1)-Sn(1)-Cl(1)**	94.6(2)	**C(1)-Sn(1)-Cl(1)**	94.84(9)
C(13)-Sn(1)-C(19)	101.0(2)	**C(1)-Sn(1)-P(1)**	78.1(3)	**C(1)-Sn(1)-P(1)**	76.3(2)	**C(1)-Sn(1)-P(1)**	76.45(9)
C(13)-Sn(1)-C(25)	122.2(2)	**C(13)-Sn(1)-C(19)**	119.1(4)	**C(13)-Sn(1)-C(14)**	116.7(5)	**C(13)-Sn(1)-C(17)**	114.93(14)
C(19)-Sn(1)-C(25)	102.0(2)	**C(13)-Sn(1)-Cl(1)**	91.7(3)	**C(13)-Sn(1)-Cl(1)**	95.5(3)	**C(13)-Sn(1)-Cl(1)**	90.42(10)
		C(13)-Sn(1)-P(1)	89.6(3)	**C(13)-Sn(1)-P(1)**	94.3(4)	**C(13)-Sn(1)-P(1)**	92.80(10)
		C(19)-Sn(1)-Cl(1)	94.1(3)	**C(14)-Sn(1)-Cl(1)**	90.4(3)	**C(17)-Sn(1)-Cl(1)**	95.02(10)
		C(19)-Sn(1)-P(1)	92.5(3)	**C(14)-Sn(1)-P(1)**	90.2(3)	**C(17)-Sn(1)-P(1)**	91.01(10)
C(19)-Sn(1)···P(1)	177.63(1)	**Cl(1)-Sn(1)-P(1)**	171.62(9)	**Cl(1)-Sn(1)-P(1)**	168.93(8)	**Cl(1)-Sn(1)-P(1)**	171.23(3)
C(9)-P(1)-C(31)	98.7(3)	**C(9)-P(1)-C(25)**	106.2(6)	**C(9)-P(1)-C(15)**	105.9(5)	**C(9)-P(1)-C(21)**	106.95(17)
C(9)-P(1)-C(34)	100.8(3)	**C(9)-P(1)-C(28)**	106.9(5)	**C(9)-P(1)-C(18)**	105.4(5)	**C(9)-P(1)-C(24)**	104.14(16)
C(31)-P(1)-C(34)	103.0(3)	**C(25)-P(1)-C(28)**	106.8(6)	**C(15)-P(1)-C(18)**	106.5(6)	**C(21)-P(1)-C(24)**	104.89(16)
		Sn(1)-P(1)-C(9)	95.6(4)	**Sn(1)-P(1)-C(9)**	95.5(3)	**Sn(1)-P(1)-C(9)**	94.46(18)
		Sn(1)-P(1)-C(25)	125.8(5)	**Sn(1)-P(1)-C(15)**	128.1(4)	**Sn(1)-P(1)-C(21)**	128.06(12)
		Sn(1)-P(1)-C(28)	113.5(4)	**Sn(1)-P(1)-C(18)**	112.6(4)	**Sn(1)-P(1)-C(24)**	114.91(12)

Table 4. Selected bond distances from X-ray crystallography and B3LYP/SBKJC/PCM optimizations [in brackets: Wiberg bond indices, WBIs]

Compd.	**P···Sn X-ray[a]**	**P···Sn opt[b]**	**Sn-Cl X-ray[a]**	**Sn-Cl opt[b]**	**μ [D][b]**
1	3.251 [0.13]	*3.337 [0.12]*	*n.a.*	*n.a.*	*3.9*
2	2.818 [0.36]	*2.877 [0.36]*	2.525 [0.50]	*2.589 [0.44]*	*12.3*

3	2.896 [0.32]	*2.869 [0.36]*	2.619 [0.47]	*2.607 [0.42]*	*13.0*
4	2.866 [0.33]	*2.929 [0.33]*	2.527 [0.49]	*2.594 [0.43]*	*12.0*

[a]X-Ray coordinates employed. [b]Fully optimised.

Additionally, the optimized Sn-Cl bond lengths are in good agreement with those observed experimentally in the solid, with WBIs of ~0.5 suggesting weaker Sn-Cl bonding as a result of the lone-pair interaction. Furthermore, the presence of the electropositive tin centre in these polar systems ensures the bonds it forms, and especially those to highly electronegative chlorine atoms, are highly ionic in character. Therefore, in addition to the contribution from covalent donor-acceptor type interactions as reflected in the high WBIs, the short P-Sn contacts observed in **2-4** may also stem from significant electrostatic [P(+)-Sn Cl(-)] type interactions. The computed atomic charges from natural population analysis,[41] *ca*. 0.9, 1.9 and -0.7 on P, Sn and Cl, respectively, confirm the polar bonding within this moiety, as do the resulting large dipole moments of the molecules (Table 4)

CONCLUSION

A combination of X-ray crystallography, solution- and solid-state NMR spectroscopy and density functional theory (DFT) calculations has been used to investigate how substituents bound to tin affect the strength of the intramolecular lone-pair P→Sn donor-acceptor interactions and thus the magnitude of spin-spin coupling constants between formally non-bonded Sn and P atoms in Acenap(SnR_3)(P^iPr_2) (R_3 = Ph_3 **1**; Ph_2Cl **2**; Me_2Cl **3**; Bu_2Cl **4**). Mono-systems **1-4** adopt similar conformations, classified as type BAA-CC for **1** and BAA-AC for **2-4**. In all four compounds, two Sn-C_R bonds align perpendicular and on opposing sides of the mean acenaphthene plane (type A) leaving the remaining Sn-C_{Ph} bond in **1** and the Sn-Cl bonds in **2-4** along the acenaphthene plane (type B). In each case this produces a *quasi*-linear Y-Sn···P three-body fragment which provides the correct geometry for promoting delocalization of the phosphorus lone-pair to an antibonding σ*(Sn−Y) orbital to form a donor-acceptor three-centre four-electron (3c-4e) type interaction. *Peri*-distances in triorganotin dichlorides **2-4** (**2** 2.815(3) Å, **3** 2.912(3) Å, **4** 2.8721(10) Å) are notably shorter than in triphenyl derivative **1** (3.2511(19) Å) suggesting the lone-pair interaction is more prevalent in these compounds due to the presence of the highly electronegative chlorine atoms which increase the Lewis-acidity of the tin centre. This is supported by substantial through-space $J(^{31}P,^{119/117}Sn)$ SSCCs observed for **2-4** (**2** 754/721 Hz; **3** 742/709 Hz; **4** 740/707 Hz), in both solution- and solid-state NMR spectra, which are notably larger than the coupling in **1** (375/355 Hz), although the latter still suggests a significant through-space interaction. DFT calculations confirm the increased covalent bonding between P and Sn in **2-4**, with notable WBIs of *ca*. 0.35 obtained, compared to 0.1 in **1**.

EXPERIMENTAL SECTION

All experiments were carried out under an oxygen- and moisture-free nitrogen atmosphere using standard Schlenk techniques and glassware. Reagents were obtained from commercial sources and used as received. Dry solvents were collected from a MBraun solvent system. Elemental analyses were performed by Stephen Boyer at the London Metropolitan University. ^1H and ^{13}C NMR spectra were recorded on a Bruker AVANCE 300 MHz spectrometer with δ(H) and δ(C) referenced to external tetramethylsilane. ^{31}P and ^{119}Sn NMR spectra were recorded on a Jeol GSX 270 MHz spectrometer with δ(P) and δ(Sn) referenced to external phosphoric acid and tetramethylstannane, respectively. Assignments of ^{13}C and ^1H NMR spectra were made with the help of H-H COSY and HSQC experiments. All measurements were performed at 25 °C. All values reported for NMR spectroscopy are in parts per million (ppm). Coupling constants (*J*) are given in Hertz (Hz). Mass spectrometry was performed by the University of St Andrews Mass Spectrometry Service. Electrospray Mass Spectrometry (ESMS) was carried out on a Micromass LCT orthogonal accelerator time of flight mass spectrometer. 5-(bromo)-6-(diisopropylphosphino)acenaphthene was prepared following a previously reported procedure.[18]

6-Diisopropylphosphinoacenaphth-5-yl-triphenyltin [Acenap($SnPh_3$)(P^iPr_2)] (1): To a solution of 5-bromo-6-diisopropylphosphinoacenapthene [Acenap(Br)(P^iPr_2)] (0.5 g, 1.43 mmol) in diethyl ether (15 mL) at -78 ºC was added dropwise a 2.5 M solution of *n*-butyllithium in hexane (0.6 mL, 1.43 mmol). The mixture was stirred at this temperature for 1 h after which a solution of triphenyltin chloride Ph_3ClSn (0.5 g, 1.43 mmol) in diethyl ether (5 mL) was added dropwise. The solution was then allowed to warm to room temperature and stirred overnight. The resulting orange suspension was washed with degassed water and the organic layer was separated, dried over magnesium sulfate and concentrated under reduced pressure. Removal of solvents *in vacuo* gave a yellow oil, which was washed with diethyl ether (5 mL) to give the title compound as a colourless solid. An analytically pure sample was obtained by recrystallisation from a saturated solution of the compound in hexane (0.64 g, 72%); m.p. 222-224°C; elemental analysis (Found: C, 69.72; H, 5.96. Calc. for $C_{36}H_{37}PSn$: C, 69.81; H, 6.02%); ^1H NMR (300 MHz, $CDCl_3$, 25°C, Me_4Si): δ = 7.84 (1 H, d, $^3J(^1H,^1H)$ = 6.9 Hz, $^3J(^1H,^{119/117}Sn)$ = 70/67, Acenap 4-H), 7.65-7.57 (6 H, m, Sn*Ph*), 7.46 (1 H, dd, $^3J(^1H,^1H)$ = 7.0 Hz, $^3J(^1H,^{31}P)$ = 3.6 Hz, Acenap 7-H), 7.28-7.15 (11 H, m, Acenap 3,8-H, Sn*Ph*), 3.35 (4 H, s, Acenap 2xCH_2), 1.80-1.61 (2 H, m, 2xP*CH*), 0.57 (6 H, dd, $^3J(^1H,^1H)$ = 6.9 Hz, $^3J(^1H,^{31}P)$ = 14.6 Hz, 2xCH_3), 0.25 (6 H, dd, $^3J(^1H,^1H)$ = 7.0 Hz, $^3J(^1H,^{31}P)$ = 11.8 Hz, 2xCH_3); ^{13}C NMR (75.5 MHz; $CDCl_3$; 25ºC; Me_4Si): δ = 141.5(s), 137.7(s, $^2J(^{13}C,^{119/117}Sn)$ = 33.3 Hz), 133.6(d, $^2J(^{13}C,^{31}P)$ = 2.7 Hz, C-7), 128.5(s), 128.1(s), 120.0(s), 119.4(s), 30.6(s, Acenap CH_2), 30.4(s, Acenap CH_2), 25.6(d, $^1J(^{13}C,^{31}P)$ = 10.4 Hz, 2xP*C*H), 19.7(d, $^2J(^{13}C,^{31}P)$ = 14.6 Hz, 2xCH_3), 18.5(d, $^2J(^{13}C,^{31}P)$ = 6.5 Hz, 2xCH_3); ^{31}P NMR (109.4 MHz; $CDCl_3$; 25ºC; H_3PO_4): δ = -31.5 (s, $J(^{31}P,^{119/117}Sn)$ = 373/355 Hz); ^{119}Sn NMR (100.7 MHz; $CDCl_3$; 25ºC; Me_4Sn): δ = -183.7 (d, $J(^{119}Sn,^{31}P)$ = 373 Hz); MS (ES^+): *m/z* 642.57 (100%, M + Na).

6-Diisopropylphosphinoacenaphth-5-yl-diphenyltin chloride [Acenap($SnPh_2Cl$)(P^iPr_2)] (2): Experimental as for compound **1** but with [Acenap(Br)(P^iPr_2)] (0.5 g, 1.43mmol), 2.5 M solution of *n*-butyllithium in hexane (0.6 mL, 1.43 mmol) and Ph_2Cl_2Sn (0.49 g, 1.43 mmol). The crude product was washed with toluene, the mixture was filtered and the toluene was removed *in vacuo*. An analytically pure sample was obtained from recrystallisation by diffusion of hexane into a saturated solution of the compound in THF (0.54 g, 65%); m.p. 214-216°C; elemental analysis (Found: C, 62.29; H, 5.51 Calc. for $C_{30}H_{32}PSnCl$: C, 62.37; H, 5.58%); ^1H NMR (300 MHz, $CDCl_3$, 25°C, Me_4Si): δ = 8.94 (1 H, d, $^3J(^1H,^1H)$ = 7.1 Hz, $^3J(^1H,^{119}Sn)$ = 83 Hz, Acenap 4-H), 7.76-7.63 (6 H, m, Sn*Ph*), 7.52-7.35 (4 H, m, Acenap 3,7-H, Sn*Ph*), 7.29-7.11 (5 H, m, Acenap 8-H, Sn*Ph*), 3.33 (4 H, s, Acenap 2xCH_2), 2.14-1.93 (2 H, m, 2xP*CH*), 0.57 (6 H, dd, $^3J(^1H,^1H)$ = 7.0 Hz, $^3J(^1H,^{31}P)$ = 16.8 Hz, 2xCH_3), 0.46 (6 H, dd, $^3J(^1H,^1H)$ = 7.0 Hz, $^3J(^1H,^{31}P)$ = 13.0 Hz, 2xCH_3); ^{13}C NMR (75.5 MHz; $CDCl_3$; 25ºC; Me_4Si): δ = 141.3(d, $^4J(^{13}C,^{31}P)$ = 6.8 Hz, $^2J(^{13}C,^{119/117}Sn)$ = 50.0 Hz, C-4), 136.4(s, $^2J(^{13}C,^{119/117}Sn)$ = 43.9

Hz), 133.6(d, $^{2}J(^{13}C,^{31}P)$ = 2.5 Hz, C-7), 129.3(s), 129.1(s), 121.3(d, $^{5}J(^{13}C,^{31}P)$ = 3.4 Hz, C-3), 119.7(d, $^{3}J(^{13}C,^{31}P)$ = 4.1 Hz, C-8), 31.1(s, Acenap CH_2), 30.6(s, Acenap CH_2), 23.7(d, $^{1}J(^{13}C,^{31}P)$ = 5.1 Hz, 2xP*C*H), 18.6(d, $^{2}J(^{13}C,^{31}P)$ = 5.1 Hz, 2xCH_3), 17.1(br s, 2xCH_3); ^{31}P NMR (109.4 MHz; $CDCl_3$; 25ºC; H_3PO_4): δ = -27.3 (s, $J(^{31}P,^{119/117}Sn)$ = 754/721 Hz); ^{119}Sn NMR (100.7 MHz; $CDCl_3$; 25ºC; Me_4Sn): δ = -241.0 (d, $J(^{119}Sn,^{31}P)$ = 754 Hz); MS (ES^+): *m/z* 542.60 (100%, M - Cl + Na).

6-Diisopropylphosphinoacenaphth-5-yl-dimethyltin chloride [Acenap(SnMe$_2$Cl)(P^{i}Pr$_2$)] (3): Experimental as for compound **1** but with [Acenap(Br)(P^{i}Pr$_2$)] (0.5 g, 1.43mmol), 2.5 M solution of *n*-butyllithium in hexane (0.6 mL, 1.43 mmol) and Me_2Cl_2Sn (0.31 g, 1.43 mmol). The crude product was washed with toluene, the mixture was filtered and the toluene was removed *in vacuo*. An analytically pure sample was obtained from recrystallisation by diffusion of hexane into a saturated solution of the compound in dichloromethane (0.3 g, 46%); m.p. 174-176°C; elemental analysis (Found: C, 53.17; H, 6.35. Calc. for $C_{20}H_{28}PSnCl$: C, 52.96; H, 6.22%); ^{1}H NMR (300 MHz, $CDCl_3$, 25°C, Me_4Si): δ = 8.67 (1 H, d, $^{3}J(^{1}H,^{1}H)$ = 7.0 Hz, $^{3}J(^{1}H,^{119/117}Sn)$ = 78 Hz, Acenap 4-H), 7.54-7.42 (1 H, m, Acenap 7-H), 7.34 (1 H, d, $^{3}J(^{1}H,^{1}H)$ = 7.0 Hz, Acenap 3-H), 7.26 (1 H, d, $^{3}J(^{1}H,^{1}H)$ = 7.1, Acenap 8-H), 3.29 (4 H, s, Acenap 2xCH_2), 2.42-2.25 (2 H, m, 2xP*CH*), 1.10-0.86 (18 H, m, 2xPCH(CH_3)$_2$, 2xSnCH_3); ^{13}C NMR (75.5 MHz; $CDCl_3$; 25ºC; Me_4Si): δ = 140.4(d, $^{4}J(^{13}C,^{31}P)$ = 6.7 Hz, C-4), 133.1(d, $^{2}J(^{13}C,^{31}P)$ = 2.5 Hz, C-7), 121.5(d, $^{5}J(^{13}C,^{31}P)$ = 2.9 Hz, C-3), 119.5(d, $^{3}J(^{13}C,^{31}P)$ = 4.3 Hz, C-8), 31.0(s, Acenap CH_2), 30.5(s, Acenap CH_2), 23.9(d, $^{1}J(^{13}C,^{31}P)$ = 5.2 Hz, 2xP*C*H), 19.7(br s, 2xPCH(CH_3)$_2$), 19.6 (br s, 2xPCH(CH_3)$_2$), 18.3(s, 2xSnCH_3); ^{31}P NMR (109.4 MHz; $CDCl_3$; 25ºC; H_3PO_4): δ = -24.4 (s, $J(^{31}P,^{119/117}Sn)$ = 742/709 Hz); ^{119}Sn NMR (100.7 MHz; $CDCl_3$; 25ºC; Me_4Sn): δ = -143.1 (d, $J(^{119}Sn,^{31}P)$ = 742 Hz); MS (ES^+): *m/z* 419.09 (100%, M-Cl).

6-Diisopropylphosphinoacenaphth-5-yl-dibutyltin chloride [Acenap(SnBu$_2$Cl)(P^{i}Pr$_2$)] (4): Experimental as for compound **1** but with [Acenap(Br)(P^{i}Pr$_2$)] (1.0 g, 2.86 mmol), 2.5 M solution of *n*-butyllithium in hexane (1.14 mL, 2.86 mmol) and Ph_2Cl_2Sn (0.87 g, 2.86 mmol). The resulting orange oil was washed with MeCN (5 mL) to give the title compound as a cream solid. An analytically pure sample was obtained by recrystallisation from a saturated solution of the compound in hexane (1.54 g, 93%); m.p. 186-188°C; elemental analysis (Found: C, 58.01; H, 7.57. Calc. for $C_{26}H_{40}PSnCl$: C, 58.07; H, 7.50%); ^{1}H NMR (300 MHz, $CDCl_3$, 25°C, Me_4Si): δ = 8.65 (1 H, d, $^{3}J(^{1}H,^{1}H)$ = 7.0 Hz, $^{3}J(^{1}H,^{119/117}Sn)$ = 70/67 Hz, Acenap 4-H), 7.51 (1 H, dd, $^{3}J(^{1}H,^{1}H)$ = 7.0, $^{3}J(^{1}H,^{31}P)$ = 5.7 Hz, Acenap 7-H), 7.37 (1 H, d, $^{3}J(^{1}H,^{1}H)$ = 7.0 Hz, Acenap 3-H), 7.28 (1 H, d, $^{3}J(^{1}H,^{1}H)$ = 7.0 Hz, Acenap 8-H), 3.35 (4 H, s, Acenap 2xCH_2), 2.42-2.30 (2 H, m, 2xP*CH*), 1.82-1.45 (8 H, m, 2xCH_2-α, 2xCH_2-β), 1.36-1.20 (4 H, m, 2xCH_2-γ), 1.06-0.92 (12 H, m, 2xPCH(CH_3)$_2$), 0.79 (6 H, t, $^{3}J(^{1}H,^{1}H)$ = 7.3 Hz, 2xCH_3-δ); ^{13}C NMR (75.5 MHz; $CDCl_3$; 25ºC; Me_4Si): δ = 140.6(d, $^{4}J(^{13}C,^{31}P)$ = 6.4 Hz, C-4), 132.8(d, $^{2}J(^{13}C,^{31}P)$ = 2.7 Hz, C-7), 121.1(d, $^{5}J(^{13}C,^{31}P)$ = 2.8 Hz, C-3), 119.2(d, $^{3}J(^{13}C,^{31}P)$ = 4.0 Hz, C-8), 30.9(s, Acenap CH_2), 30.4(s, Acenap CH_2), 29.0(s, $^{2}J(^{13}C,^{119/117}Sn)$ = 31.8 Hz, 2xCH_2-β), 27.3(s, $^{3}J(^{13}C,^{119/117}Sn)$ = 38.3 Hz, 2xCH_2-γ), 24.0(d, $^{1}J(^{13}C,^{31}P)$ = 3.4 Hz, 2xP*C*H), 23.7(d, $^{3}J(^{13}C,^{31}P)$ = 25.6 Hz, 2xCH_2-α), 19.7(d, $^{2}J(^{13}C,^{31}P)$ = 10.1 Hz, 2xPCH(CH_3)$_2$), 18.2 (br s, 2xPCH(CH_3)$_2$), 14.1(s, 2xCH_3-δ); ^{31}P NMR (109.4 MHz; $CDCl_3$; 25ºC; H_3PO_4): δ = -23.9 (s, $J(^{31}P,^{119/117}Sn)$ = 740/707); ^{119}Sn NMR (100.7 MHz; $CDCl_3$; 25ºC; Me_4Sn): δ = -118.4 (d, $J(^{119}Sn,^{31}P)$ = 740 Hz); MS (ES^+): *m/z* 503.19 (100%, M-Cl).

SOLID-STATE NMR EXPERIMENTAL DETAILS

^{31}P and ^{119}Sn solid-state NMR were performed using a Bruker Avance III spectrometer operating at a magnetic field strength of 9.4 T, corresponding to Larmor frequencies of 161.9 (^{31}P) and 149.2 (^{119}Sn) MHz. Experiments were carried out using conventional 4-mm MAS probes, with MAS rates between 12.5 and 14 kHz. Chemical shifts are referenced relative to 85% H_3PO_4 at 0 ppm using the isotropic resonance of solid BPO_4 at –29.6 ppm as a secondary reference, and to $(CH_3)_4Sn$ at 0 ppm using the isotropic resonance of solid SnO_2 at –604.3 ppm as a secondary reference. For ^{31}P, spectra were acquired using a π/2 pulse lengths of 3.1 μs and a recycle interval of 30 s. For ^{119}Sn, spectra were acquired using either using a π/2 pulse lengths of 1.9 μs and a recycle interval of 30 s, or by transfer of magnetisation from ^{1}H in a cross polarization (CP) experiment. In CP, transverse magnetization was obtained using optimized contact pulse durations of 1 ms, and continuous wave (cw) ^{1}H decoupling during acquisition, and a recycle interval of 10 s. The position of the isotropic resonances within the spinning sidebands patterns were unambiguously determined by recording a second spectrum at a higher MAS rate (isotropic resonances are marked with a * in Figure 3). A more detailed description of the experimental parameters for individual materials is given in the Supporting Information.

CRYSTAL STRUCTURE ANALYSES

X-ray crystal structures for **1** and **2** were determined at −148(1) °C using a Rigaku MM007 high-brilliance RA generator (Mo Kα radiation, confocal optic) and Saturn CCD system. At least a full hemisphere of data was collected using ω scans. Intensities were corrected for Lorentz, polarization, and absorption. Data for compounds **3-4** were collected at −180(1) °C using a Rigaku MM007 high-brilliance RA generator (Mo Kα radiation, confocal optic) and Mercury CCD system. At least a full hemisphere of data was collected using ω scans. Data for the complexes analyzed was collected and processed using CrystalClear (Rigaku).[42] Structures were solved by direct methods[43] and expanded using Fourier techniques.[44] Non-hydrogen atoms were refined anisotropically. Hydrogen atoms were refined using the riding model. All calculations were performed using the CrystalStructure[45] crystallographic software package except for refinement, which was performed using SHELXL-97.[46] These X-ray data can be obtained free of charge via www.ccdc.cam.ac.uk/conts/retrieving.html or from the Cambridge Crystallographic Data Centre, 12 Union Road, Cambridge CB2 1EZ, UK; fax (+44) 1223-336-033; e-mail: deposit@ccdc.cam.ac.uk. CCDC Nos 992224-992228.

COMPUTATIONAL DETAILS

The same methods were used as in our previous study on acenaphthene tin derivatives,[24] i.e. geometries were fully optimised in the gas phase at the B3LYP[47] level using the Compact Effective Potential by Stevens et al along with the SBKJC 2s3p2d valence basis[48] and 6-31G(d) basis elsewhere. Wiberg bond indices[29] were obtained in a natural bond orbital analysis[41] at the same level. Experimental structures from X-ray crystallography were used as the starting geometry. All five structures were reoptimized with the same methods and basis sets using the PCM implementation of Tomasi and co-workers[40] (employing the united-atom UFF radii and the parameters of THF), denoted PCM. The computations were performed using the Gaussian 03 suite of programs.[49]

ASSOCIATED CONTENT

Supporting Information

Solid-state NMR data; tables and figures; X-ray crystallographic data; tables and figures; Computational data; Text file of all computed molecule Cartesian coordinates in a format for convenient

Visualization; This material is available free of charge via the internet at http://pubs.acs.org.

AUTHOR INFORMATION

Corresponding Author

*E-mail: jdw3@st-andrews.ac.uk.

Notes

The authors declare no competing financial interests.

ACKNOWLEDGMENT

Elemental analyses were performed by Stephen Boyer at the London Metropolitan University. Mass spectrometry was performed by Caroline Horsburgh at the University of St. Andrews Mass Spectrometry Service. Calculations were performed using the EaStCHEM Research Computing Facility maintained by Dr. H. Früchtl. The work in this project was supported by the Engineering and Physical Sciences Research Council (EPSRC). M.B. wishes to thank EaStCHEM and the University of St Andrews for support.

REFERENCES

(1) For example, see: (a) Katz, H. E. *J. Am. Chem. Soc*. **1985**, *107*, 1420. (b) Alder, R. W.; Bowman, P. S.; Steel, W. R. S.; Winterman, D. R. *Chem. Commun.* **1968**, 723. (c) Costa, T.; Schimdbaur, H. *Chem. Ber*. **1982**, *115*, 1374. (d) Karaçar, A.; Freytag, M.; Thönnessen, H.; Omelanczuk, J.; Jones, P. G.; Bartsch, R.; Schmutzler, R. *Heteroat. Chem.* **2001**, *12*, 102. (e) Glass, R. S.; Andruski, S. W.; Broeker, J. L.; Firouzabadi, H.; Steffen, L. K.; Wilson, G. S. *J. Am. Chem. Soc*. **1989**, *111*, 4036. (f) Fuji, T.; Kimura, T.; Furukawa, N. *Tetrahedron Lett*. **1995**, *36*, 1075. (g) Schiemenz, G. P. *Z. Anorg. All. Chem*. **2002**, 628, 2597. (h) Corriu, R. J. P.; Young, J. C. *In Hypervalent Silicon Compounds, in Organic Silicon Compounds*; Patai, S., Rappoport, Z., Eds.; John Wiley & Sons Ltd.: Chichester, UK, **1989**; Vols. 1 and 2.

(2) (a) Coulson, C. A.; Daudel, R.; Robertson, J. M. *Proc., R. Soc. London Ser. A.* **1951**, *207*, 306. (b) Cruickshank, D. W. *Acta Crystallogr*. **1957**, *10*, 504. (c) Brock, C. P.; Dunitz, J. D. *Acta Crystallogr., Sect. B* **1982**, *38*, 2218. (d) Oddershede, J.; Larsen, S. *J. Phys. Chem. A* **2004**, *108*, 1057.

(3) Hazell, A. C.; Hazell, R. G.; Nørskov-Lauritsen, L.; Briant, C. E.; Jones, D. W. *Acta Crystallogr., Sect. C* **1986**, *42*, 690.

(4) Balasubramaniyan, V. *Chem. Rev.* **1966**, *66*, 567.

(5) Kilian, P.; Knight, F. R.; Woollins, J. D. *Chem. Eur. J.* **2011**, *17*, 2302.

(6) Bondi, A. *J. Phys. Chem.* **1964**, *68*, 441.

(7) (a) Schmidbaur, H.; Öller, H.-J.; Wilkinson, D. L.; Huber, B.; Müller, G. *Chem. Ber*. **1989**, *122*, 31. (b) Fujihara, H.; Furukawa, N. *J. Mol. Struct*. **1989**, *186*, 261. (c) Fujihara, H.; Akaishi, R.; Erata, T.; Furukawa, N. *J. Chem. Soc., Chem. Commun.* **1989**, 1789. (d) Handal, J.; White, J. G.; Franck, R.W.; Yuh, Y. H.; Allinger, N. L. *J. Am. Chem. Soc*. **1977**, *99*, 3345. (e) Blount, J. F.; Cozzi, F.; Damewood, J. R.; Iroff, D. L.; Sjöstrand, U.; Mislow, K. *J. Am. Chem. Soc.* **1980**, *102*, 99. (f) Anet, F. A. L.; Donovan, D.; Sjöstrand, U.; Cozzi, F.; Mislow, K. *J. Am. Chem. Soc*. **1980**, *102*, 1748. (g) Hounshell, W. D.; Anet, F. A. L.; Cozzi, F.; Damewood, J. R., Jr.; Johnson, C. A.; Sjöstrand, U.; Mislow, K. *J. Am. Chem. Soc*. **1980**, *102*, 5941. (h) Schrock, R.; Angermaier, K.; Sladek, A.; Schmidbaur, H. *Organometallics* **1994**, *13*, 3399.

(8) (a) Nakanishi, W.; Hayashi, S.; Toyota, S. *Chem. Commun*. **1996**, 371. (b) Nakanishi, W.; Hayashi, S.; Sakaue, A.; Ono, G.; Kawada, Y. *J. Am. Chem. Soc.* **1998**, *120*, 3635. (c) Nakanishi, W.; Hayashi, S.; Toyota, S. *J. Org. Chem.* **1998**, *63*, 8790. (d) Hayashi, S.; Nakanishi, W. *J. Org. Chem.* **1999**, *64*, 6688. (e) Nakanishi, W.; Hayashi, S.; Uehara, T. *J. Phys. Chem. A* **1999**, *103*, 9906. (f) Nakanishi, W.; Hayashi, S.; Uehara, T. *Eur. J. Org. Chem*. **2001**, 3933. (g) Nakanishi, W.; Hayashi, S. *Phosphorus Sulfur Silicon Relat. Elem.* **2002**, *177*, 1833. (h) Nakanishi, W.; Hayashi, S.; Arai, T. *Chem. Commun*. **2002**, 2416. (i) Hayashi, S.; Nakanishi, W. *J. Org. Chem.* **2002**, *67*, 38. (j) Nakanishi, W.; Hayashi, S.; Itoh, N. *Chem. Commun*. **2003**, 124. (k) Hayashi, S.; Wada, H.; Ueno, T.; Nakanishi, W. *J. Org. Chem.* **2006**, *71*, 5574. (l) Hayashi, S.; Nakanishi, W. *Bull. Chem. Soc. Jpn*. **2008**, *81*, 1605.

(9) (a) Meinwald, J.; Dauplaise, D.; Wudl, F.; Hauser, J. J. *J. Am. Chem. Soc.* **1977**, *99*, 255. (b) Ashe III, A. J.; Kampf, J. W.; Savla, P. M. *Heteroatom Chem.* **1994**, *5*, 113. (c) Lanfrey, M. *C. R. Acad. Sci.* **1911**, *152*, 92. (d) Price, W. B.; Smiles, S. *J. Chem. Soc.* **1928**, 2372. (e) Zweig, A.; Hoffman, A. K. *J. Org. Chem.* **1965**, *30*, 3997. (f) Kilian, P.; Slawin, A. M. Z.; Woollins, J. D. *Dalton Trans.* **2006**, 2175. (g) Kilian, P.; Philp, D.; Slawin, A. M. Z.; Woollins, J. D. *Eur. J. Inorg. Chem.* **2003**, 249.

(10) Kilian, P.; Knight, F. R.; Woollins, J. D. *Coord. Chem. Rev.* **2011**, *255*, 1387.

(11) (a) Chuit, C.; Reyé, C. *Eur. J. Inorg. Chem*. **1998**, 1847. (b) Bushuk, S. B.; Carré, F. H.; Guy, D. M. H.; Douglas, W. E.; Kalvinkovskaya, Y. A.; Klapshina, L. G.; Rubinov, A. N.; Stupak, A. P.; Bushuk, B. A. *Polyhedron* **2004**, *23*, 2615. (c) Chauhan, M.; Chuit, C.; Fruchier, A.; Reyé, C. *Inorg. Chem.* **1999**, *38*, 1336. (d) Carré, F. H.; Chauhan, M.; Chuit, C.; Corriu, R. J. P.; Reyé, C. *Phosphorus Sulfur Silicon Relat. Elem.* **1997**, *123*, 181.

(12) (a) Schiemenz, G. P. *Z. Anorg. Allg. Chem*. **2002**, *628*, 2597. (b) Schiemenz, G. P. *Z. Naturforsch. B* **2006**, *61*, 535. (c) Schiemenz, G. P.; Nather, C.; Porksen, S. *Z. Naturforsch. B* **2003**, *58*, 59. (d) Schiemenz, G. P.; Nather, C.; Porksen, S. *Z. Naturforsch. B* **2003**, *58*, 663. (e) Schiemenz, G. P.; Nather, C.; Porksen, S. *Z. Naturforsch. B* **2003**, *58*, 715. (f) Schiemenz, G. P. *Phosphorus Sulfur Silicon Relat. Elem*. **2009**, *184*, 2247. (g) Schiemenz, G. P. *Phosphorus Sulfur Silicon Relat. Elem*. **2000**, *163*, 185. (h) Schiemenz, G. P.; Bukowski, R.; Eckholtz, L.; Varnskühler, B. *Z. Naturforsch. B* **2000**, *55*, 12. (i) Schiemenz, G. P.; Porksen, S.; Dominiak, P. M.; Wozniak, K. *Z. Naturforsch. B* **2002**, *57*, 8. (j) Dominiak, P. M.; Petersen, S. Schiemenz, B.; Schiemenz, G. P.; Wozniak, K. *J. Mol. Struct*. **2005**, *751*, 172.

(13) Schiemenz, G. P.; Porksen, S.; Nather, C. *Z. Naturforsch. B* **2000**, *55*, 841.

(14) Carré, F. H.; Chuit, C.; Corriu, R. J. P.; Douglas, W. E.; Guy, D. M. H.; Reyé, C. *Eur. J. Inorg. Chem*. **2000**, 647.

(15) (a) Chandrasekaran, A.; Timosheva, N. V.; Day, R. O.; Holmes, R. R. *Inorg. Chem*. **2000**, *39*, 1338. (b) Hellwinkel, D.; Lindner, W.; Wilfinger, H.-J. *Tetrahedron Lett*. **1969**, *10*, 3423. (c) Hellwinkel, D.; Lindner, W.; Wilfinger, H.-J. *Chem. Ber*. **1974**, *107*, 1428. (d) Day, R. O.; Holmes, R. R. *Inorg. Chem.* **1980**, *19*, 3609.

(16) Panda, A.; Mugesh, G.; Singh, H. B.; Butcher, R. J. *Organometallics* **1999**, *18*, 1986-1993.

(17) (a) Beckmann, J.; Bolsinger, J.; Duthie, A.; Finke, P. *Dalton. Trans*. **2013**, *42*, 12193. (b) Beckmann, J.; Bolsinger, J.; Duthie, A. *Chem. Eur. J*. **2011**, *17*, 930.

(18) (a) Wawrzyniak, P.; Slawin, A. M. Z.; Woollins, J. D.; Kilian, P. *Dalton Trans*. **2010**, *39*, 85. (b) Wawrzyniak, P.; Fuller, A. L.; Slawin, A. M. Z.; Kilian, P. *Inorg. Chem.* **2009**, *48*, 2500. (c) Surgenor, B. A.; Bühl, M.; Slawin, A. M. Z.; Woollins, J. D.; Kilian, P. *Angew. Chem. Int. Ed*. **2012**, *51*, 10150.

(19) Jastrzebski, J. T. B. H.; Boersma, J.; Esch, P. M.; van Koten, G. *Organometallics* **1991**, *10*, 930.

(20) (a) Knight, F. R.; Fuller, A. L.; Bühl, M.; Slawin, A. M. Z.; Woollins, J. D. *Chem. Eur. J*. **2010**, *16*, 7503. (b) Knight, F. R.; Fuller, A. L.; Bühl, M.; Slawin, A. M. Z.; Woollins, J. D. *Chem. Eur. J*. **2010**, 16, 7605.

(21) Knight, F. R.; Fuller, A. L.; Bühl, M.; Slawin, A. M. Z.; Woollins, J. D. *Chem. Eur. J*. **2010**, 16, 7617.

(22) Aschenbach, L. K.; Knight, F. R.; Randall, R. A. M.; Cordes, D. B.; Baggott, A.; Bühl, M.; Slawin, A. M. Z.; Woollins, J. D. *Dalton Trans.* **2012**, *41*, 3141.

(23) (a) Knight, F. R.; Fuller, A. L.; Bühl, M.; Slawin, A. M. Z.; Woollins, J. D. *Inorg. Chem*. **2010**, *49*, 7577. (b) Knight, F. R.; Athukorala Arachchige, K. S.; Randall, R. A. M.; Bühl, M.; Slawin, A. M. Z.; Woollins, J. D. *Dalton Trans.* **2012**, *41*, 3154.

(24) Lechner, M.-L.; Athukorala Arachchige, K. S.; Randall, R. A. M.; Knight, F. R.; Bühl, M.; Slawin, A. M. Z.; Woollins, J. D. *Organometallics* **2012**, *31*, 2922.

(25) Knight, F. R.; Randall, R. A. M.; Athukorala Arachchige, K. S.; Wakefield, L.; Griffin, J. M.; Ashbrook, S. E.; Bühl, M.; Slawin, A. M. Z.; Woollins, J. D. *Inorg. Chem.* **2012**, *51*, 11087.

(26) Bühl, M. Knight, F. R.; Křístková, A.; Malkin Ondík, I.; Malkina, O. L.; Randall, R. A. M.; Slawin, A. M. Z.; Woollins, J. D. *Angew. Chem*. **2013**, *125*, 2555. *Angew. Chem. Int. Ed*. **2013**, *52*, 2495.

(27) Diamond, L. M.; Knight, F. R.; Athukorala Arachchige, K. S.; Randall, R. A. M.; Bühl, M.; Slawin, A. M. Z.; Woollins, J. D. *Eur. J. Inorg. Chem*. **2014**, 1512.

(28) Stanford, M. W.; Knight, F. R.; Athukorala Arachchige, K. S.; Sanz Camacho, P.; Ashbrook, S. E.; Bühl, M.; Slawin, A. M. Z.; Woollins, J. D. *Dalton Trans.* **2014**, 43, 6548.
(29) Wiberg, K. B. *Tetrahedron* **1968,** *24*, 1083.
(30) (a) Kemp, W. *NMR in Chemistry; A Multinuclear Introduction*, Macmillan Education Ltd., Hampshire, England, **1986**. (b) Parish, R. V. *NMR, NQR, EPR, and Mössbauer Spectroscopy in Inorganic Chemistry*, Ed. Burgess, J.; Ellis Horwood, Chichester, England, **1990**.
(31) (a) Ernst, L.; Sakhaii, P. *Magn. Reson. Chem.* **2000**, *38*, 559. (b) Ernst, L.; Ibrom, K. *Angew. Chem. Int. Ed. Engl.* **1995**, *34*, 1881.
(32) (a) Mallory, F. B.; Mallory, C. W.; Butler, K. E.; Beth Lewis, M.; Qian Xia, A.; Luzik, Jr., E. D.; Fredenburgh, L. E.; Ramanjulu, M. M.; Van, Q. N.; Francl, M. M.; Freed, D. A.; Wray, C. C.; Hann, C.; Nerz-Stormes, M.; Carroll, P. J.; Chirlian, L. E. *J. Am. Chem. Soc*. **2000**, *122*, 4108. (b) Peralta, J. E.; Barone, V.; Contreras, R. H.; Zaccari, D. G.; Snyder, J. P. *J. Am. Chem. Soc*. **2001**, *123*, 9162.
(33) Reiter, S. A.; Nogai, S. D.; Karaghiosoff, K.; Schmidbaur, H. *J. Am. Chem. Soc*. **2004**, *126*, 15833.
(34) Nakanishi, W.; Hayashi, S. *Chem. Eur. J.* **2008**, *14*, 5645.
(35) Cornils, B.; Herrman, W. *Applied homogeneous Catalysis with Organometallic Compounds*; Wiley-VCH: Weinheim, **2000**.
(36) For example: Wong, C. Y.; Kennepohl, D. K.; Cavell, R. G. *Chem. Rev*. **1996**, *96*, 1917.
(37) Freitag, S.; Krebs, K. M.; Henning, J.; Hirdler, J.; Schubert, H.; Wesemann, L. *Organometallics* **2013**, 32, 6785.
(38) Nagy, P.; Szabó, D.; Kapovits, I.; Kucsman, Á.; Argay, G.; Kálmán, A. *J. Mol. Struct.* **2002**, *606*, 61.
(39) (a) Balas, V. I.; Banti, C. N.; Kourkoumelis, N.; Hadjikakou, S. K.; Geromichalos, G. D.; Sahpazidou, D.; Male, L.; Hursthouse, M. B.; Bednarz, B.; Kubicki, M.; Charalabopoulos, K.; Hadjiliadis, N. *Aust. J. Chem.* **2012**, *65*, 1625. (b) Greene, P. T.; Bryan, R. F. *J. Chem. Soc. A*, **1971**, 2549. (c) Davies, A. G.; Milledge, H. J.; Puxley, D. C.; Smith, P. J. *J. Chem. Soc. A* **1970**, 2862. (d) Sawyer, J. F. *Acta Crystallogr., Sect.C: Cryst. Struct. Commun*. **1988**, *44*, 633.
(40) As implemented in Gaussian 03: (a) Barone, V.; Cossi, M.; Tomasi, J. *J. Comput. Chem.* **1998**, *19*, 404. (b) Cossi, M.; Scalmani, G.; Rega, N.; Barone, V. *J. Chem. Phys*. **2002**, *117*, 43. (c) Cossi, M.; Crescenzi, O. *J. Chem. Phys.* **2003**, *19*, 8863.
(41) Reed, A. E.; Curtiss, L. A.; Weinhold, F. *Chem. Rev*. **1988,** *88*, 899.
(42) CrystalClear 1.6: Rigaku Corporation, 1999. CrystalClear Software User's Guide, Molecular Structure Corporation, (c) 2000. Flugrath, J. W. P. *Acta Crystallogr*., *Sect. D* **1999**, *D55*, 1718.
(43) SIR97: Altomare, A.; Burla, M.; Camalli, M.; Cascarano, G.; Giacovazzo, C.; Guagliardi, A.; Moliterni, A.; Polidori, G.; Spagna, R. *J. Appl. Cryst.* **1999**, *32*, 115.
(44) DIRDIF99: Beurskens, P. T.; Admiraal, G.; Beurskens, G.; Bosman, W. P.; de Gelder, R.; Israel, R.; Smits, J. M. M. 1999. The DIRDIF-99 program system, Technical Report of the Crystallography Laboratory, University of Nijmegen, The Netherlands.
(45) CrystalStructure 3.8.1: Crystal Structure Analysis Package, Rigaku and Rigaku/MSC (2000-2006). 9009 New Trails Dr. The Woodlands TX 77381 USA.
(46) SHELX97: Sheldrick, G. M. *Acta Crystallogr.*, *Sect. A* **2008**, *64*, 112.
(47) (a) Becke, D., *J. Chem. Phys.* **1993,** *98*, 5648. (b) Lee, C.; Yang, W.; Parr, R. G. *Phys. Rev. B* **1988**, *37*, 785.
(48) (a) Labello, N. P.; Ferreira, A. M.; Kurtz, H. A., *J. Comput. Chem.* **2005,** 26, 1464. (b) Stevens, W. J.; Krauss, M.; Basch, H.; Jasien, P. G. *Can. J. Chem.* **1992,** *70*, 612.
(49) Pople, J. A.; *et al*. Gaussian 03, Revision E.01; Gaussian, Inc.: Wallingford, CT, 2004 (for a full citation see ref S1, Supporting Information).

Authors are required to submit a graphic entry for the Table of Contents (TOC) that, in conjunction with the manuscript title, should give the reader a representative idea of one of the following: A key structure, reaction, equation, concept, or theorem, etc., that is discussed in the manuscript. Consult the journal's Instructions for Authors for TOC graphic specifications.

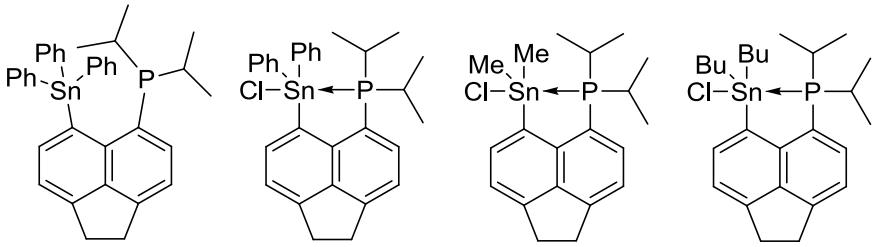

J_{PSn} = 373 Hz
P...Sn WBI 0.13

J_{PSn} = 754 Hz
P...Sn WBI 0.36

J_{PSn} = 742 Hz
P...Sn WBI 0.32

J_{PSn} = 740 Hz
P...Sn WBI 0.33